Hindawi
Wireless Communications and Mobile Computing
Volume 2022, Article ID 3786839, 15 pages
https://doi.org/10.1155/2022/3786839

Research Article

Outage Performance Analysis of CR-NOMA Based on Incremental Relay

Chuanwang Song, Haisong Zhang, Yuming Li, Hao Zhang, Enyu Li, and Keyong Hu

School of Information and Control Engineering, Qingdao University of Technology, Qingdao 266520, China

Correspondence should be addressed to Chuanwang Song; songchw@163.com

Received 2 August 2022; Revised 16 September 2022; Accepted 27 September 2022; Published 10 October 2022

Academic Editor: Xingwang Li

Considering the problem of limited spectrum and relay resources, we proposed a scheme using incremental relay protocol to improve the secondary network outage performance. Firstly, a CR-NOMA network system model combined with incremental relay protocol is constructed. The primary network and the secondary network share the same relay for communication. When the user of the secondary network fails to receive information, the node closest to the shared relay is selected as an incremental relay to assist transmission. Secondly, the exact expressions of outage probability and throughput are derived, and the Monte Carlo method is used to verify the results. Based on the outage probability and throughput of the secondary network, the transmission power ratio between primary and secondary networks and the power distribution of shared relay are optimized. Compared with the average power allocation schema, it is proved that the optimized schema has advantages in improving the outage performance and throughput. Through simulation and analysis of outage performance with or without using incremental relay protocol, it is concluded that adding an incremental relay in the shared relay network can reduce the probability of system outage and improve network reliability.

1. Introduction

With the increase of wireless multimedia applications and the widely popularized of intelligent terminals, wireless communications are developing rapidly. In the meanwhile, the number of users and instrumentation accessing to the communication network surges constantly in order that the spectrum resources become increasingly nervous. Thus, faced with the increasing shortage of spectrum resources and the large-scale connection of intelligent terminals, a way to meet users' requirements of exploitation spectrum resources has become an important topic in communication analysis [1–3]. Nonorthogonal multiple access (NOMA) has been considered an efficient resolution to the shortage of spectrum resources. To eliminate the generated cochannel interference, the successive interference cancellation (SIC) is used on the receiver end to achieve correct demodulation [4, 5]. Previous studies have proved that NOMA can support more users to access the same spectrum of resources. Its upstream and downstream links can obtain 20% and 30% system capacity gain, respectively [6]. In [7], the impact of residual transceiver hardware impairments on cooperative NOMA networks was investigated, where generic α-μ fading channel is considered. In addition, in [8], the authors studied the effective capacity of the simultaneously transmitting and reflecting reconfigurable intelligent surface aided NOMA networks, illustrating the clear advantages of using NOMA over orthogonal multiple access (OMA) for the overall system. The power allocation problem of NOMA has been widely concerned. In [9], a user grouping and power allocation algorithm based on the NOMA system is proposed to ensure the stability of SIC, and it also avoids serious performance degradation caused by error propagation. In [10], the authors studied the optimal power

allocation among users which guarantees quality of service for weighted sum-rate maximization in downlink NOMA networks.

Another technology that can solve the shortage of spectrum resources and improve the utilization of spectrum is cognitive radio (CR). On the premise that the communication between authorized users is not affected, that is, the primary network communicates normally; unlicensed or secondary users are permitted to use bands allocated to the licensed or primary users [11, 12]. The combination of NOMA and CR, also known as CR-NOMA, which is conducive to spectrum reuse, can meet the increasing requirements of users and provide services for a large number of consumers [13]. The introduction of CR-NOMA provides more advantages for wireless communication. In [14], the authors investigated the deployment of an unmanned aerial vehicle as a relay in CR-NOMA network. In [15], the authors have proved that the cooperation between V2X (vehicle-to-everything) and CR-NOMA is beneficial to serve group vehicles. Considering the loss in the communication process, the performance of CR-NOMA in Rayleigh fading channel under residual interference considering incomplete channel state information and continuous interference cancellation is studied in [16]. Due to the difference between Rayleigh channel and reality, the authors in [17] studied the performance of CR-NOMA under incomplete channel state information in Nakagami fading channels. In addition, the authors in [18] proposed a low-complexity PSO algorithm to improve the security energy efficiency of the downlink underlying CR-NOMA system. In [19], the authors integrated CR, NOMA, and multiple-input multiple-output (MIMO) and proposed a MIMO-based CR-NOMA communication system, which is proved superior to the existing MIMO-NOMA and CR-NOMA systems in improving spectral efficiency. Moreover, in [20], a multihop cooperative transmission protocol was proposed. When the destination cannot decode the source message accurately, the most recent successful relay is selected for retransmission.

To further improve the capacity gain of the system and provide connections for more users, the authors researchers in [21, 22] investigated a dual-hop cooperative relaying scheme based on NOMA, in which two sources communicate with their corresponding receiver ends in the same frequency band via a common relay, respectively. Using the shared relay can provide more communication opportunities for secondary network users. Providing large-scale connectivity to dense users is one of the main goals of future radio access [5]. In the CR-NOMA relay sharing network, it is worthy of further study on how to meet the interference power constraint of the primary user and improve the transmission performance of the secondary network without increasing the transmission power [23].

In recent years, the incremental relay (IR) protocol has been widely used to improve the spectral efficiency of cooperative wireless networks. When the cooperating receiver end can successfully decode the message, IR does not have to retransmit the message. The work in [24, 25] applied IR to the NOMA network and evaluated the user communication performance under incomplete SIC, which showed a significant improvement in performance compared to the scheme without increment relay. However, these systems do not involve CR technology, which can improve spectrum efficiency and save spectrum resources. The authors in [26] analyzed a CR-NOMA system based on the overlay mode of energy collection and proposed two cooperative spectrum sharing schemes based on the IR protocol using the amplify-and-forward (AF) and decode-and-forward (DF) relaying strategies. Compared with direct transmission and orthogonal multiple access schemes, higher throughput and energy efficiency can be achieved. Considering that both the primary network and the secondary network initiate information transmission simultaneously, the underlay mode should be adopted. The authors in [27] studied the performance of the primary network and the secondary network in the underlay mode with the help of assistance of incremental amplify-and-forward relay and proposed a power control coefficient to balance the performance of the two networks. However, when the secondary network sends information, it is easy to cause interference to the primary network in underlay mode. Therefore, it is necessary to consider the interference temperature limit of the primary users and limit the transmitting power of the secondary network.

In this paper, we investigate the effect of IR protocol on the performance of CR-NOMA in cooperative relay sharing. IR is used to assist the communication of secondary networks. Our main contributions are summarized below:

(1) We introduce the concept of relay sharing to CR-NOMA networks. The primary network allows the secondary network to use its licensed spectrum, and in exchange the secondary network needs to provide relays to assist the primary network in communicating. IR protocol is introduced in the network, and the node closest to the shared relay serves as the incremental relay

(2) The exact expressions of outage probability and throughput are derived analytically, and the correctness of the expressions is verified by simulation results. To improve the outage probability and throughput compromise performance of the secondary network under the condition of ensuring the normal communication of the primary network, the power distribution parameters are optimized

(3) For a fair comparison with the schema without IR, we devise a cooperative network that does not use an IR employing CR-NOMA. It is shown that the proposed scheme can effectively improve the outage performance and throughput of the secondary network, especially when the signal-to-noise ratio (SNR) is low

2. System Model

We consider an underlay CR-NOMA network as shown in Figure 1, which consists of a primary network (PN) and a secondary network (SN). PN includes a primary transmitter (PT) and a primary user (PU). Likewise, SN consists of a

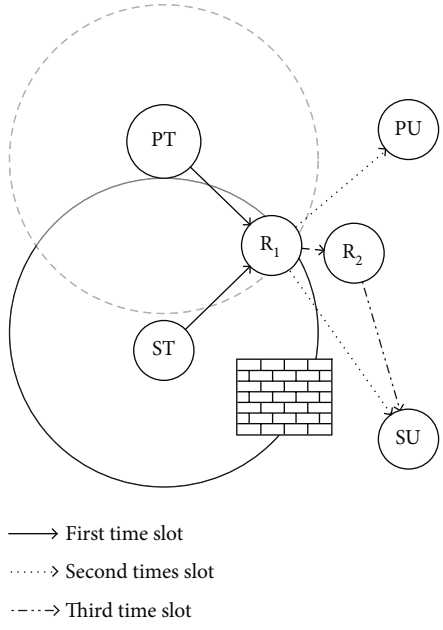

Figure 1: CR-NOMA shared relay network based on IR.

secondary transmitter (ST) and a secondary user (SU). PN allows SN to use its own spectrum resources, and in return PN borrows the SN's relays to communicate. We assume that the direct link from ST to SU does not exist due to physical obstacles or poor channel conditions. To improve the performance of the SN, the node closest to R_1 (i.e.,R_2) is selected as the IR. After SU decodes the message from R_1, it returns a message (NACK or ACK), indicating whether the message from R_1 to SU is successfully decoded. Then, the system dynamically adjusts the transmission mode based on the feedback result. When the ACK signal is fed back, R_2 no longer participates in the communication. Instead, when the NACK signal comes back, R_2 recodes x_2 and sends it to SU.

In this paper, we assume that each of the above terminals cannot simultaneously send and receive signals (i.e., half-duplex transmission). DF strategy and SIC technology are used in the network to receive users' messages and decode them. In addition, all channels suffer quasistatic Rayleigh fading. The channel coefficient between each node is represented by h_{ij}, which satisfies the complex Gaussian distribution with parameters of $\lambda_{ij} = d_{ij}^{-m}$. According to [25], d_{ij} is defined as the ratio between the actual distance and the standard distance between the sender and the receiver, which is called the normalized distance. The link distance $d_{ij} \in \{d_{PR_1}, d_{SR_1}, d_{R_1P}, d_{R_1S}, d_{R_1R_2}, d_{R_2S}\}$ denotes the distance between links PT-R_1, ST-R_1, R_1-PU, R_1-SU, R_1-R_2, and R_2-SU, respectively. The parameter m is the path loss variable, which is a function of carrier frequency, environment, obstacle, etc., usually ranging from 3 to 5. Furthermore, the noise is additive white Gaussian noise (AWGN). We further assume that all receivers can perfectly access the local CSI, i.e., R_1, PU, and SU have instantaneous CSI of the links PT-R_1 and ST-R_1, link R_1-PU, and links R_1-ST and R_2-ST, respectively [28].

The first phase corresponds to the NOMA uplink, with PT and ST sending x_1 and x_2 to R_1, respectively. The mathematical expectation of the sent message is $E[|x_1|^2] = E[|x_2|^2] = 1$. The transmitting power of the primary transmitter is represented as P_T, and that of the second transmitter as κP_T. It is expected that $\kappa < 1$ because PN contributes spectrum in communication, and the PU has higher QoS to ensure reliable information transmission of the PU. According to the NOMA uplink [20], R_1 decodes x_1 with good channel status information first using SIC technology. Therefore, the received signal-to-interference-plus-noise ratio (SINR) for symbol x_1 is written as

$$\gamma_{x_1}^{R_1} = \frac{\rho_T \left|h_{PR_1}\right|^2}{\kappa\rho_T \left|h_{SR_1}\right|^2 + 1}, \tag{1}$$

where $\rho_T = P_T/\sigma^2$. Then, R_1 performs SIC to obtain the symbol x_2; the SINR can be written as

$$\gamma_{x_2}^{R_1} = \kappa\rho_T \left|h_{SR_1}\right|^2, \tag{2}$$

where h_{PR_1} and h_{SR_1} denote the channel coefficients of channels PT-R_1 and ST-R_1, respectively.

In the second phase, R_1 broadcasts the reencoded information to PU, SU, and R_2, which is a downlink NOMA system. According to the principle of downlink NOMA, the information sent by R_1 after reencoding is written as $Z = \sqrt{\psi P_{R_1}} x_1 + \sqrt{(1-\psi)P_{R_1}} x_2$, where ψ is the power distribution factor of signals of PU and SU on relay R_1. Since PU is a high-priority NOMA receiver end, a higher power value is assigned to the PU to ensure normal communication with PN. P_{R_1} denotes the transmission power at R_1. Let $\rho_{R_1} = P_{R_1}/\sigma^2$, and R_1 transmits a superimposed composite signal

$$y_j = h_{ij}\left(\sqrt{\psi P_{R_1}} x_1 + \sqrt{(1-\psi)P_{R_1}} x_2\right) + n_k. \tag{3}$$

Let $h_{ij} \in \{h_{R_1P}, h_{R_1S}, h_{R_1R_2}\}$ indicate the channel coefficients of links R_1-PU, R_1-SU, and R_1-R_2. The parameter $n_k \in \{n_1, n_2, n_3\}$ indicates the AWGN of the PU, SU, and R_2, respectively.

According to NOMA protocol, the PU decodes the signal x_1 using SIC technology. Therefore, the SINR received at PU associated with x_1 is obtained as

$$\gamma_{x_1}^{PU} = \frac{\psi\rho_{R_1} \left|h_{R_1P}\right|^2}{(1-\psi)\rho_{R_1} \left|h_{R_1P}\right|^2 + 1}. \tag{4}$$

The SU first decodes x_1 with x_2 as interference, whose SINR is obtained as

$$\gamma_{x_1}^{SU} = \frac{\psi\rho_{R_1} \left|h_{R_1S}\right|^2}{(1-\psi)\rho_{R_1} \left|h_{R_1S}\right|^2 + 1}. \tag{5}$$

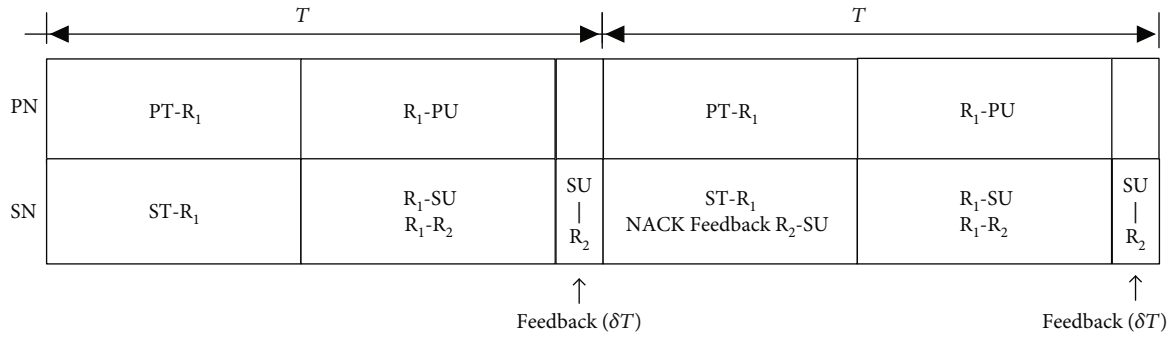

Figure 2: Timeslot allocation.

Then, SU decodes its signal x_2, whose SINR can be given as

$$\gamma_{x_2}^{SU} = (1-\psi)\rho_{R_1}\left|h_{R_1S}\right|^2. \tag{6}$$

If the SINR of R_1-SU exceeds a certain threshold, SU can decode x_2 successfully. In this case, the SU sends an ACK signal to R_2. Furthermore, R_2 does not participate in the subsequent communications. Conversely, if the decoding fails, the IR assists the SN to transmit information, and SU sends a NACK signal to R_2. Both ACK and NACK signals are fixed information set manually. Assuming that the time occupied by each feedback is δT (the feedback time is very short and the delay can be ignored), the timeslot allocation is shown in Figure 2.

The SINR of x_2 decoded at R_2 is written as

$$\gamma_{x_2}^{R2} = (1-\psi)\rho_{R_1}\left|h_{R_1S}\right|^2 = \frac{(1-\psi)\rho_{R_1}\left|h_{R_1R_2}\right|^2}{\psi\rho_{R_1}\left|h_{R_1R_2}\right|^2 + 1}. \tag{7}$$

Then, R_2 reencodes the information x_2 of the SN and sends it to SU. At the same time, the transmitters of both the PN and SN start to send the information of the next time slot to R_1. This is to ensure $T/2$ time per phase of PN regardless of whether the IR is involved in the transmission, while ignoring the feedback time. The signal SU received is written as $y = \sqrt{P_{r2}}x_2h_3 + n$, where P_{r2} represents the transmitting power at R_2. To ensure normal communication on the PN, the interference to the active network must not exceed the threshold Q. In this case, P_{r2} is defined as

$$P_{r2} = \min\left\{\frac{Q}{|h_{SP}|^2}, P_{R_2}\right\}, \tag{8}$$

where h_{SP} is the coefficient of the interference channel from PN at R_2 and its parameter λ_{SP} satisfies the complex Gaussian distribution. P_{R_2} stands for maximum transmitting power of the relay R_2. Therefore, the SINR of SU concerning x_2 is defined as

$$\gamma_{x_2}^{R_2\longrightarrow SU} = \frac{P_{r2}\left|h_{R_2S}\right|^2}{\sigma^2} = \min\left\{\frac{Q_{th}}{\left|h_{sp}\right|^2}, \rho_{R_2}\right\}\left|h_{R_2S}\right|^2, \tag{9}$$

where the power parameter satisfies $Q_{th} = Q/\sigma^2$ and $\rho_{R_2} = P_{R_2}/\sigma^2$.

3. Performance Analysis

In this section, the outage probability and throughput are characterized for the proposed system under Rayleigh fading.

3.1. Outage Probability. To improve the reliability of information transmission on the SN, R_2 is selected as the IR to assist transmission as it is closest to the shared relay R_1. Since the SINR threshold is a fixed function of channel capacity, $\gamma_{th}^{x_1}$ represents the SINR threshold of the PU and $\gamma_{th}^{x_2}$ denotes the SINR threshold of the SU. The probability of outage at R_1 at the first phase can be obtained as

$$\text{Pout1} = 1 - \Pr\left\{\gamma_{x_1}^{R_1} \geq \gamma_{th}^{x_1}, \gamma_{x_2}^{R_1} \geq \gamma_{th}^{x_2}\right\}. \tag{10}$$

The second phase involves the process of R_1 broadcasting information to the user and the process of R_2 auxiliary transmission. Therefore, the outage probability of PN in the second phase is given as

$$\text{Pout2\_}PU = 1 - \Pr\left\{\gamma_{x_1}^{PU} \geq \gamma_{th}^{x_1}\right\}. \tag{11}$$

Theorem 1. *The expression of the outage probability of the PN can be written as*

$$\text{Pout}, PU = \begin{cases} 1 - \dfrac{\lambda_{PR_1} e^{\left(-\left(\left(\gamma_{th}^{x_1}+\gamma_{th}^{x_1}\gamma_{th}^{x_2}\right)/\rho_T\lambda_{PR_1}\right)-\left(\gamma_{th}^{x_2}/\kappa\rho_T\lambda_{SR_1}\right)-\left(\gamma_{th}^{x_1}/\left(\lambda_{R_1P}\psi\left(1+\gamma_{th}^{x_1}\right)\rho_{R_1}-\gamma_{th}^{x_1}\rho_{R_1}\lambda_{R_1P}\right)\right)\right)}}{\lambda_{PR_1} + \kappa\lambda_{SR_1}\gamma_{th}^{x_1}}, & \psi > \dfrac{\gamma_{th}^{x_1}}{1+\gamma_{th}^{x_1}}, \\ 1, \quad \text{otherwise.} \end{cases} \tag{12}$$

Proof. See Appendix A. □

Similarly, the outage probability of the SN in the second phase can be given as

$$\begin{aligned}\text{Pout2\_}SU = 1 &- \Pr\left\{\gamma_{x_1}^{SU} \geq \gamma_{th}^{x_1}, \gamma_{x_2}^{SU} \geq \gamma_{th}^{x_2}\right\} \\ &- \left(\left(1 - \Pr\left\{\gamma_{x_1}^{SU} \geq \gamma_{th}^{x_1}, \gamma_{x_2}^{SU} \geq \gamma_{th}^{x_2}\right\}\right)\right. \\ &\left.\times \Pr\left\{\gamma_{x_2}^{R_2} \geq \gamma_{th}^{x_2}, \gamma_{x_2}^{R_2 \longrightarrow SU} \geq \gamma_{th}^{x_2}\right\}\right).\end{aligned} \tag{13}$$

Theorem 2 provides the outage probability of SU when both phases are considered.

Theorem 2. *The expression of outage probability of when $\psi < (1/(1+\gamma_{th}^{x_2}))$ can be written as (14). Otherwise, the outage probability is equal to 1.*

$$\begin{aligned}Pout, SU = 1 - &\frac{\lambda_{PR_1} e^{-\left(\left(\gamma_{th}^{x_1} + \gamma_{th}^{x_1}\gamma_{th}^{x_2}\right)/\rho_T \lambda_{PR_1}\right) - \left(\gamma_{th}^{x_2}/\kappa\rho_T\lambda_{SR_1}\right)}}{\lambda_{PR_1} + \kappa\lambda_{SR_1}\gamma_{th}^{x_1}} \\ &\times \left(1 - \left(1 - e^{-\theta/\rho_{R_1}\lambda_{R_1 S}}\right)\right. \\ &\times \left(1 - e^{-\left(1/\rho_{R_1}\lambda_{R_1 S}\right)\left(\gamma_{th}^{x_2}/\left((1-\psi)\rho_{R_1} - \gamma_{th}^{x_2}\psi\rho_{R_1}\right)\right) - \left(\gamma_{th}^{x_2}/\lambda_{R_2 S}\rho_{R_2}\right)}\right. \\ &\left.\left.\times \left(1 - \frac{\lambda_{SP}\gamma_{th}^{x_2}}{\lambda_{SP}\gamma_{th}^{x_2} + Q_{th}\lambda_{R_2 S}} e^{-Q_{th}\gamma_{th}^{x_2}/\lambda_{SP}\gamma_{th}^{x_2}\rho_{R_2}}\right)\right)\right),\end{aligned} \tag{14}$$

where $\theta = \max\left(\gamma_{th}^{x_1}/(\psi - \gamma_{th}^{x_1}(1-\psi)), \gamma_{th}^{x_2}/(1-\psi)\right)$.

Proof. See Appendix B. □

Because of the approximation of e^x and $1 + x$, the asymptotic expression of (14) can be expressed as

$$\begin{aligned}\text{Pout}_{\text{SU}}^{\text{Approx}} = 1 - \Delta_1 &\left(1 - \frac{\Delta_2}{\rho_T}\right) \\ &\times \left(1 - \frac{\theta}{\rho_{R_1}\lambda_{R_1 S}} \times \left(1 - \Delta_4 + \frac{\Delta_3\Delta_4}{\lambda_{R_1 R_2}\rho_{R_1}} + \frac{\gamma_{th}^{x_2}\Delta_4}{\lambda_{R_2 S}\rho_{R_2}}\right)\right),\end{aligned} \tag{15}$$

where $\Delta_4 = (\rho_{R_2} Q_{th}\lambda_{R_2 S} + Q_{th}\gamma_{th}^{x_2})/(\rho_{R_2}(\lambda_{SP}\gamma_{th}^{x_2} + Q_{th}\lambda_{R_2 S}))$, $\Delta_3 = \gamma_{th}^{x_2}/((1-\psi) - \gamma_{th}^{x_2}\psi)$, $\Delta_2 = ((\gamma_{th}^{x_1} + \gamma_{th}^{x_1}\gamma_{th}^{x_2})\kappa\lambda_{SR_1} + \gamma_{th}^{x_1}\lambda_{PR_1})/\lambda_{PR_1}\kappa\lambda_{SR_1}$, and $\Delta_1 = \lambda_{PR_1}/(\lambda_{PR_1} + \kappa\lambda_{SR_1}\gamma_{th}^{x_1})$.

According to (12) and (14), when $x \longrightarrow 0$, $e^x \longrightarrow 1$, we can obtain the approximate expression of the outage probability of PU and SU by Corollary 3.

Corollary 3. *The bounds of outage probability of PU and SU at a high SNR ($\rho \longrightarrow \infty$) can be calculated as*

$$Pout_{\infty} \approx 1 - \frac{\lambda_{PR_1}}{\lambda_{PR_1} + \kappa\lambda_{SR_1}\gamma_{th}^{x_1}}. \tag{16}$$

To make a fair comparison with the networks that do not use IR protocol, we build a cooperative network employing CR-NOMA without IR. Similarly, the PN and SN use the same relay to communicate. When the SINR of SU decoding is less than the threshold, the system interrupts.

Theorem 4. *The outage probability of the SN without IR can be expressed as*

$$Pout = 1 - \frac{\lambda_{PR_1}}{\lambda_{PR_1} + \kappa\lambda_{SR_1}\gamma_{th}^{x_1}} e^{-\left(\left(\gamma_{th}^{x_1} + \gamma_{th}^{x_1}\gamma_{th}^{x_2}\right)/\rho_T\lambda_{PR_1}\right) - \left(\gamma_{th}^{x_2}/\kappa\rho_T\lambda_{SR_1}\right) - \left(\theta/\rho_{R_1}\lambda_{R_1 S}\right)}. \tag{17}$$

Proof. See Appendix C. □

3.2. Throughput. According to the time slot allocation in Figure 2, each transmission time of PN is T, while the transmission time of the SN in the first transmission cycle can be computed as

$$T_{\text{ID}} = \begin{cases} T, & \gamma_{x_2}^{\text{SU}} \geq \gamma_{th}^{x_2}, \\ \dfrac{T - \delta T}{2} + T = \dfrac{3T - \delta T}{2}, & \gamma_{x_2}^{\text{SU}} < \gamma_{th}^{x_2}. \end{cases} \tag{18}$$

Let $H1 = \Pr\{\gamma_{x_1}^{\text{SU}} \geq \gamma_{th}^{x_1}, \gamma_{x_2}^{\text{SU}} \geq \gamma_{th}^{x_2}\}$; then, Theorem 5 provides the throughput of SU according to [29].

Theorem 5. *The throughput of the SN can be expressed as*

$$\begin{aligned}Thr_{ID}\text{\_}SU &= \frac{TR_S \times (1 - Pout\text{\_}SU)}{H1 \times T + (1 - H1) \times ((3T - \delta T)/2)} \\ &= \frac{2R_S \times (1 - Pout\text{\_}SU)}{e^{-\theta/\rho_{R_1}\lambda_{R_1 S}} \times (\delta - 1) + (3 - \delta)},\end{aligned} \tag{19}$$

where H1 represents $H1 = \Pr\{\gamma_{x_1}^{SU} \geq \gamma_{th}^{x_1}, \gamma_{x_2}^{SU} \geq \gamma_{th}^{x_2}\}$, *and* $\theta = \max\left(\gamma_{th}^{x_1}/(\psi - \gamma_{th}^{x_1}(1-\psi)), \gamma_{th}^{x_2}/(1-\psi)\right)$. *In addition, R denotes the transmission rate of users in the SN.*

Similarly, the asymptotic expression of throughput in (19) can be expressed as

$$\text{Thr}_{\text{SU}}^{\text{Approx}} = \frac{2R_S \times (1 - \text{Pout\_SU})}{\left(1 - \left(\theta/\rho_{R_1}\lambda_{R_1 S}\right)\right) \times (\delta - 1) + (3 - \delta)}. \tag{20}$$

4. Optimization of Power Distribution Factor

In this section, the compromise performance between the outage probability and throughput of the SN is considered, and then the optimal power allocation scheme is obtained by ensuring the successful transmission of PN.

According to the accurate outage probability expressions of the PN and the SN in (12) and (14), it can be concluded that the transmitter power of the SN and the power distribution factor of the common relay R_1 affect the outage performance of the SN. Meanwhile, the throughput of the SU in (19) is taken into consideration. The outage probability

and throughput tradeoff performance of the SN can be improved on the premise of ensuring the success of PN transmission by a reasonable allocation of parameters. The problem above is formulated as (21), where $\mathrm{Thr}_{\mathrm{ID}}$/Pout represents the outage probability and throughput tradeoff performance of the SN. Constraints $C1$ and $C2$ are used to ensure the correct execution of SIC and that the PN's information can be successfully decoded by both R_1 and the PU. $C1$ implies that R_1 can decode user signals successfully.

$$\begin{aligned}
&\max_{\kappa,\psi} \quad \left\{\frac{\mathrm{Thr}_{\mathrm{ID}}}{\mathrm{Pout}}\right\} = \max_{\kappa,\psi}\left\{\frac{2R_S\times(1-\mathrm{Pout_SU})}{\left(e^{-\theta/\rho_{R_1}\lambda_{R_1S}}\times(\delta-1)+3-\delta\right)\mathrm{Pout_SU}}\right\}\\
&\text{s.t.}C1: \gamma_{x_1}^{R_1}\geq\gamma_{th}^{x_1}, \gamma_{x_2}^{R_1}\geq\gamma_{th}^{x_2}\\
&\quad C2: \gamma_{x_1}^{PU}\geq\gamma_{th}^{x_1}\\
&\quad C3: \psi\left(1+\gamma_{th}^{x_1}\right)-\gamma_{th}^{x_1}\geq 0, 1-\psi\left(1+\gamma_{th}^{x_2}\right)\geq 0\\
&\quad C4: 0<\kappa<1.
\end{aligned} \tag{21}$$

Likewise, $C2$ means that the information transmission of the PU must meet its QoS requirements; that is, SINR cannot be lower than the threshold. Further, $C3$ is the necessary condition for the formulation of (12) and (14). $C4$ ensures that the PN can have higher transmission power. Due to the independence of channels, the optimization problem can be divided into two subproblems according to the two phases of communication.

4.1. The Optimization Problem of the First Phase. The optimization objective of the first phase is to find the right power ratio κ between the SN and the PN so that R_1 can successfully decode signals from both transmitters. According to (10) and (19), the objective function of the first phase can be formulated as $\min_{\kappa}\{\mathrm{Pout1}\}$. After reduction, the problem in the first phase is formulated as

$$\begin{aligned}
&\min_{\kappa} \quad \left\{-\frac{1}{\lambda_{PR_1}+\kappa\lambda_{SR_1}\gamma_{th}^{x_1}}e^{-\gamma_{th}^{x_2}/\kappa\rho_T\lambda_{SR_1}}\right\}\\
&\text{s.t.} \quad C1: \frac{\rho_T\left|h_{PR_1}\right|^2}{\kappa\rho_T\left|h_{PR_1}\right|^2+1}\geq\gamma_{th}^{x_1}\\
&\qquad C2: \kappa\rho_T\left|h_{SR_1}\right|^2\geq\gamma_{th}^{x_2}\\
&\qquad C3: \kappa<1.
\end{aligned} \tag{22}$$

where $A=\gamma_{th}^{x_2}/\rho_T\lambda_{SR_1}$, $B=\lambda_{SR_1}\gamma_{th}^{x_1}$, $\Delta=\sqrt{(AB)^2+4AB\lambda_{PR_1}}$, $\kappa_{\min}=\gamma_{th}^{x_2}/\rho_T\left|h_{SR_1}\right|^2$, and $\kappa_{\max}=(\rho_T\left|h_{PR_1}\right|^2-\gamma_{th}^{x_1})/\gamma_{th}^{x_1}\rho_T\left|h_{SR_1}\right|^2$.

Theorem 6. *The optimal solution to the first phase can be expressed as*

$$\kappa^*=\begin{cases}\kappa_{\min}, & \dfrac{AB+\Delta}{2B}<\kappa_{\min},\\ \kappa_{\max}, & \dfrac{AB+\Delta}{2B}>\kappa_{\max},\\ \dfrac{AB+\Delta}{2B}, & \kappa\in[\kappa_{\min},\kappa_{\max}],\end{cases} \tag{23}$$

Proof. See Appendix D. □

4.2. The Optimization Problem of the Second Phase. After determining the value of κ, the outage probability in the first phase can be regarded as a fixed value. Therefore, $(\lambda_{PR_1}/(\lambda_{PR_1}+\kappa\lambda_{SR_1}\gamma_{th}^{x_1}))e^{-((\gamma_{th}^{x_1}+\gamma_{th}^{x_1}\gamma_{th}^{x_2})/\rho_T\lambda_{PR_1})-(\gamma_{th}^{x_2}/\kappa\rho_T\lambda_{SR_1})}$ is a constant. Then, the second problem is analyzed to find the most appropriate value of ψ, so as to achieve the optimal compromise performance between the interruption and throughput of the SU based on successful transmission on the PN. The problem of the second phase can be formulated as (24).

$$\begin{aligned}
&\max_{\psi} \quad \left\{\frac{\mathrm{Thr}_{\mathrm{ID}}}{\mathrm{Pout}}\right\} = \max_{\psi}\left\{\frac{3R_S\times(1-\mathrm{Pout_SU})}{\left(e^{-\theta/\rho_{R_1}\lambda_{R_1S}}\times(\delta-1)+3-\delta\right)\mathrm{Pout_SU}}\right\}\\
&\text{s.t.}C1: \gamma_{x_1}^{PU}\geq\gamma_{th}^{x_1}\\
&\quad C2: \frac{\gamma_{th}^{x_1}}{1+\gamma_{th}^{x_1}}\leq\psi<\frac{1}{1+\gamma_{th}^{x_2}}.
\end{aligned} \tag{24}$$

Theorem 7. *Thr_{ID} and 1/Pout increase or decrease equally as ψ changes. They are both increasing in case $\psi<((\gamma_{th}^{x_1}+\gamma_{th}^{x_1}\gamma_{th}^{x_2})/(\gamma_{th}^{x_2}+\gamma_{th}^{x_1}\gamma_{th}^{x_2}+\gamma_{th}^{x_1}))$ and decreasing in case $\psi\geq((\gamma_{th}^{x_1}+\gamma_{th}^{x_1}\gamma_{th}^{x_2})/\gamma_{th}^{x_2}+\gamma_{th}^{x_1}\gamma_{th}^{x_2}+\gamma_{th}^{x_1})$.*

Proof. See Appendix E. □

It is known from Theorem 7 that the objective function $\mathrm{Thr}_{\mathrm{ID}}$/Pout in the second phase increases in case $\psi<((\gamma_{th}^{x_1}+\gamma_{th}^{x_1}\gamma_{th}^{x_2})/(\gamma_{th}^{x_2}+\gamma_{th}^{x_1}\gamma_{th}^{x_2}+\gamma_{th}^{x_1}))$ and decreases in case $\psi\geq((\gamma_{th}^{x_1}+\gamma_{th}^{x_1}\gamma_{th}^{x_2})/(\gamma_{th}^{x_2}+\gamma_{th}^{x_1}\gamma_{th}^{x_2}+\gamma_{th}^{x_1}))$.

Theorem 8. *Considering C1 and C2 in (22), the value range of the power distribution factor ψ can be determined. The optimized power distribution factor can be expressed as*

$$\psi^*=\begin{cases}\dfrac{\gamma_{th}^{x_1}+\gamma_{th}^{x_1}\gamma_{th}^{x_2}}{\gamma_{th}^{x_2}+\gamma_{th}^{x_1}\gamma_{th}^{x_2}+\gamma_{th}^{x_1}}, & \dfrac{\chi\gamma_{th}^{x_2}}{(1-\chi)\left(1+\gamma_{th}^{x_2}\right)}<\gamma_{th}^{x_1}\leq\dfrac{1}{1+\gamma_{th}^{x_2}},\\ \dfrac{1}{1+\gamma_{th}^{x_2}}, & \gamma_{th}^{x_1}>\dfrac{1}{1+\gamma_{th}^{x_2}},\\ \chi, & otherwise,\end{cases} \tag{25}$$

Table 1: Network model parameters.

Parameter	Value
Noise variance	$\sigma^2 = 1$
Distance factor	$d_{1r} = 0.5, d_{2r} = 0.5, d_{r1} = 1, d_{r2} = 2.5, d_{12} = 1, d_3 = 1$
Power distribution factor	$\kappa < 1, \gamma_{th}^{x_1}/1 + \gamma_{th}^{x_1} < \psi < 1/1 + \gamma_{th}^{x_2}$
User SINR threshold	$\gamma_{th}^{x_1} = 0.1, \gamma_{th}^{x_2} = 0.3$
Path loss exponent	3

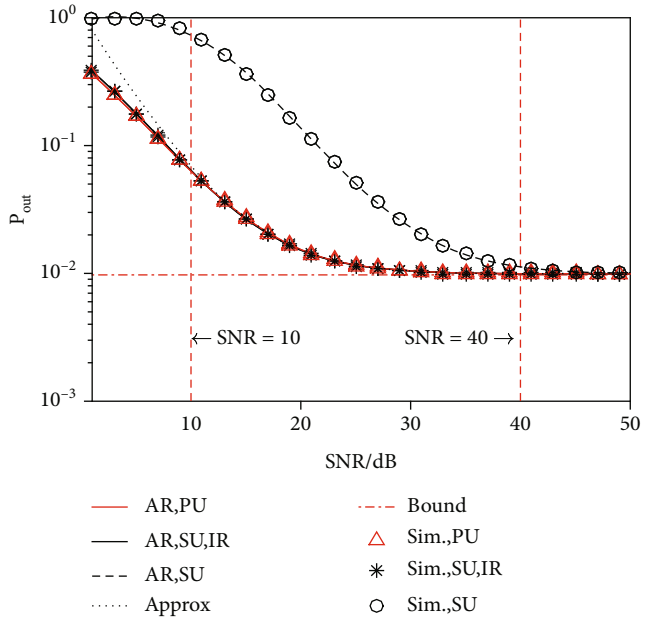

Figure 3: Theory and simulation value of outage probability in network system.

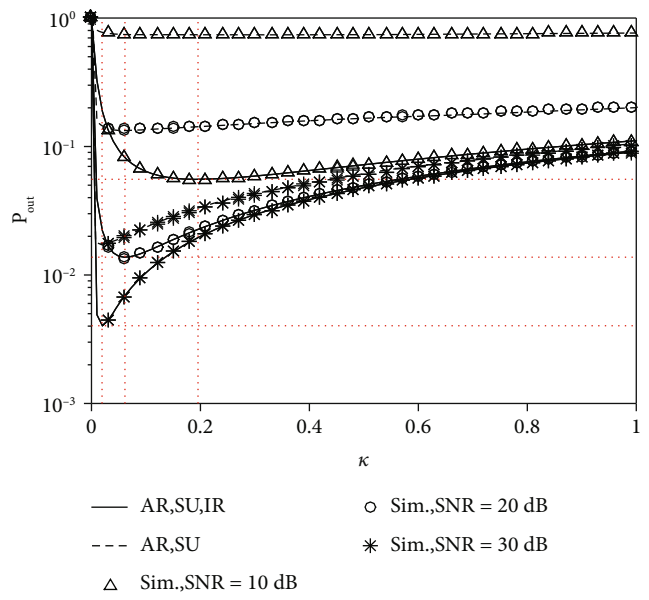

Figure 4: Variation of outage probability of SN affected by κ.

where χ *depicts the value of* $(\gamma_{th}^{x_1}/(\rho_{R_1}|h_{R_1P}|^2 + \gamma_{th}^{x_1}\rho_{R_1}|h_{R_1P}|^2)) + (\gamma_{th}^{x_1}/(1 + \gamma_{th}^{x_1}))$.

Proof. See Appendix F. □

5. Results and Discussion

In this paper, the IR is used to assist the information transmission of the SN in the scenario where the PN and SN share the common relay. The outage probability and throughput of the IR transmission strategy are deduced and analyzed. Furthermore, the network is simulated and verified in Rayleigh fading channel. Network model parameters are shown in Table 1 referring to the parameter settings in [25].

In the following, we denote the "Analytical Result" by "AR" and the Monte Carlo simulation results by "Sim."

5.1. Outage Probability. In Figure 3, we present the change of system outage probability with SNR of CR-NOMA network based on IR protocol and compare the outage probability with that of the network system without an IR. Monte Carlo simulation curves coincide with the theoretical results, which proves the correctness of the theoretical results. As shown in Figure 3, the outage probability decreases with the increase of SNR, while the slope of the curve decreases, indicating that the change degree of the system outage probability gradually decreases. Finally, when the SNR is large enough, the probability of network outage tends to a certain value regardless whether there is an IR or not. The reason is that the IR does not affect the process of information transmission at R_1. When the SNR value is less than 10 dB, the outage probability of the SN system without increment relay is very high, which is close to 1, while the proposed scheme can obtain better outage performance. At low SNR, the outage probability of the system assisted by the IR is always lower than that of the system without IR. When the SNR is greater than 40 dB, the system outage probability with or without IR assistance tends to be consistent. For the PN, the outage probability is always no higher than that of the cognitive network, indicating that adding an IR can improve the outage performance of the SN without affecting the performance of the PN.

Figure 4 shows the variation of system outage probability with κ, where κ represents the ratio of transmission power of the SN to that of the PN. The outage probability of the SN decreases rapidly at first, and then increases gradually with the increase of κ. The reason for that change is that when

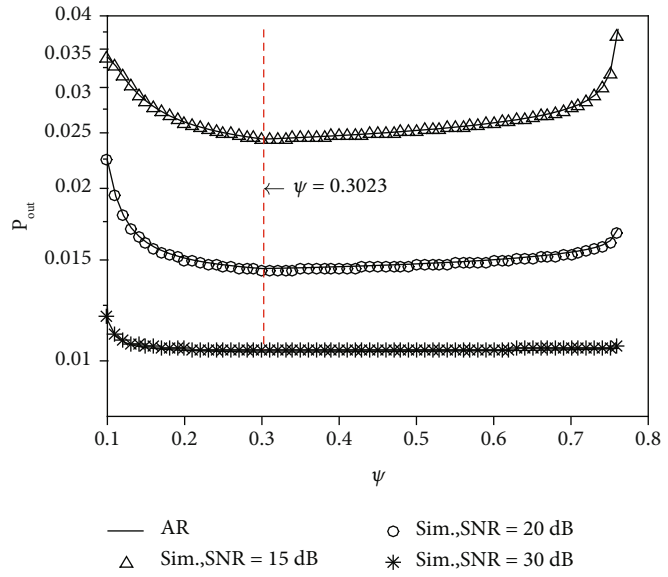

Figure 5: Variation of outage probability of SN under power allocation factor ψ.

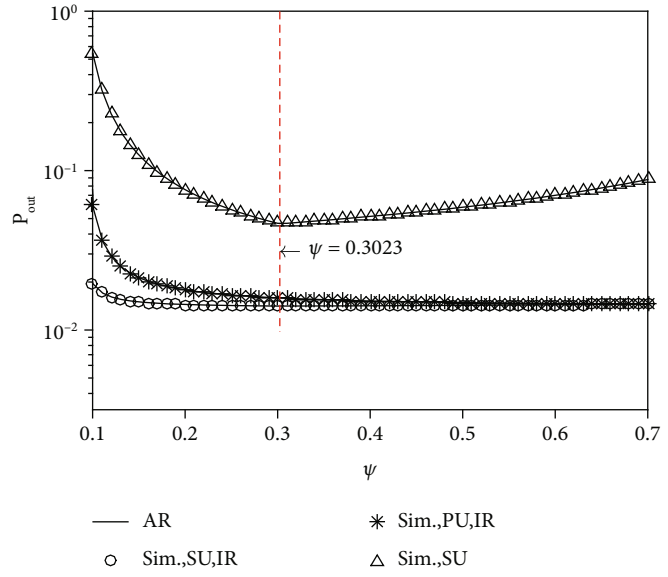

Figure 6: Comparison of outage probability with or without IR.

the value of κ is extremely low, the transmission power of the SN is too small to decode the SN information and the communication will be interrupted. With the increase of κ, the PN information is interfered by SN information. When the power and interference are low, the probability of system outage is low, while when the transmission power is high, the influence of interference is relatively obvious.

So the probability of system outage increases. With different SNR, the κ value corresponding to the minimum outage probability is different; however, it is specifically adequate to $AB + \Delta/2B$. In addition, the larger the SNR is, the smaller the κ value for optimal outage performance of the system is. Compared with the network without IR, the proposed scheme can obtain better outage performance even at lower transmitting power of the SN transmitter.

Figure 5 shows the change of outage probability with power distribution factor ψ of the SN. Together with the same SNR, with the increase of ψ, the system outage probability of the SN decreases first and then increases. The ψ values are equal when the outage probability is minimized under different SNR (the simulation results show that $\psi =$ 0.3023, which minimizes the outage probability). This is exactly equal to $(\gamma_{th}^{x_1} + \gamma_{th}^{x_1}\gamma_{th}^{x_2})/(\gamma_{th}^{x_2} + \gamma_{th}^{x_1}\gamma_{th}^{x_2} + \gamma_{th}^{x_1})$ obtained in (23), which proves the correctness of the proposed power distribution scheme.

When $\psi < 0.3023$, the system outage probability decreases gradually since the increased power is used to transmit SN's information. While when $\psi > 0.3023$, the outage probability increases since SU needs to decode the primary information first. This requires sufficient power to

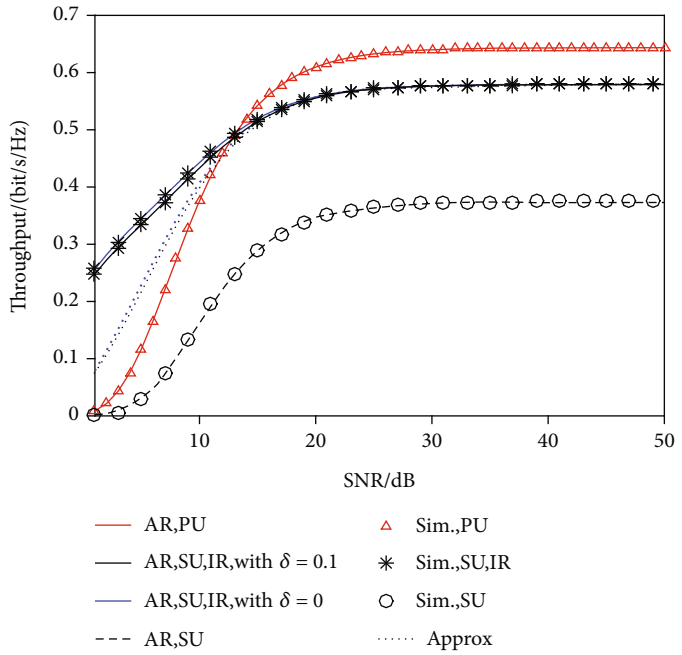

Figure 7: Theory and simulation value of throughput in network system.

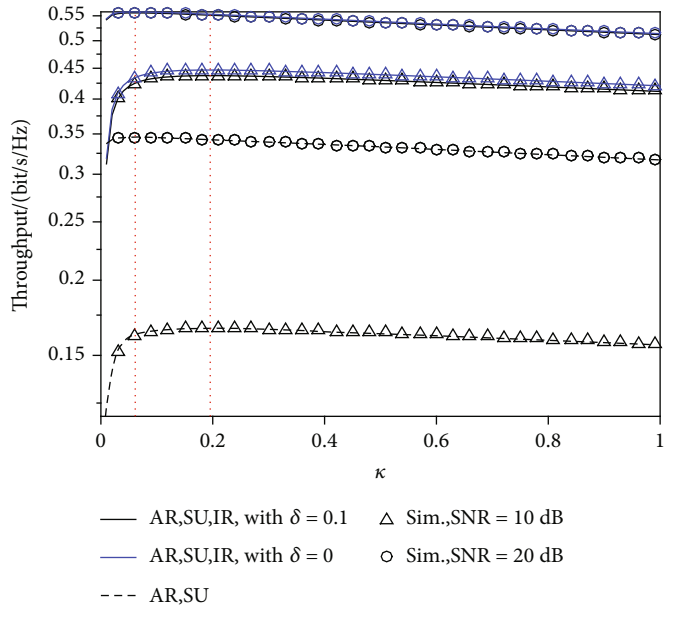

Figure 8: Variation of throughput of SN affected by κ.

allocate to primary information. Furthermore, with the increase of the outage probability, the slope of the curve becomes smaller and the variation trend tends to be stable, indicating that with the increase of SNR, the influence of ψ gradually decreases.

To compare and analyze the performance of cooperative communication schemes with and without IR protocol, Figure 6 simulates the outage probability of transmission schemes with or without IR when SNR = 20 dB. The results show that whether there is IR or not, the increase of ψ makes the outage probability decrease first and then increase. In contrast to the scheme without IR, outage probability presents fewer variations with IR assistance. In the proposed scheme, the system outage probability is always lower than that in the scenario without R_2. When $\psi = 0.3023$, the outage probability of the scheme with or without IR is the minimum. In this case, the outage probability of the system assisted by the IR is 2.25% lower than that without the IR.

Simultaneously, we simulate the change of PN outage probability with ψ. The outage probability of the PN

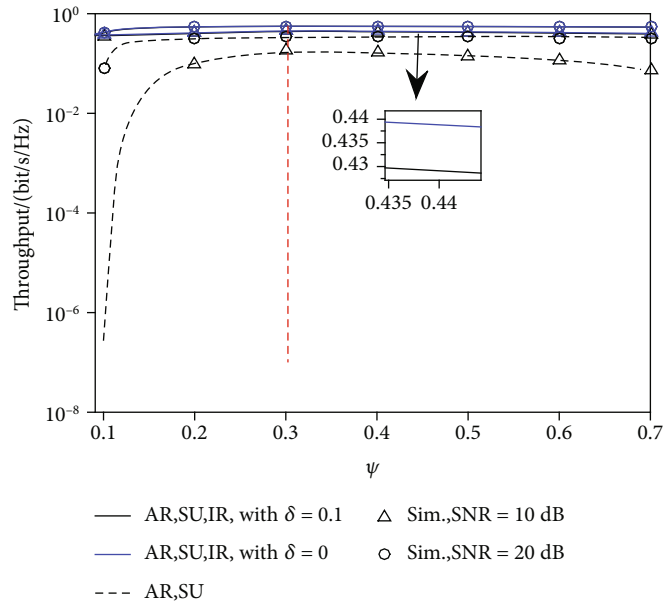

Figure 9: Variation of throughput of SN under power allocation factor ψ.

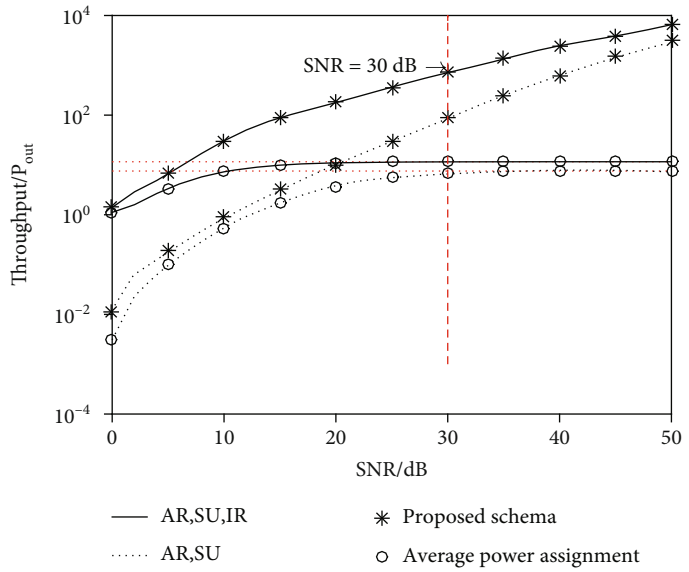

Figure 10: Comparison of outage probability between optimized schema and average power distribution schema.

decreases with the increase of ψ. There is no significant difference between the outage probability of the PN and that of the improved SN. Therefore, it is shown that the proposed scheme can improve the outage performance of the SN while ensuring the outage performance of the PN.

5.2. Throughput. Throughput indicates the number of messages successfully transmitted per unit of time. In Figure 7, the throughput variation with SNR of CR-NOMA network system based on IR protocol was showed. Furthermore, it is compared with the network system without IR. The Monte Carlo simulation curve is consistent with the theoretical results, which proves the correctness of the theoretical results. When the SNR is low, the throughput of the PN is lower than that of the SN. The throughput of the PN increases faster and gradually exceeds that of the SN.

As shown in Figure 7, the throughput increases with the increase of SNR. Finally, when the SNR is large enough, the throughput of the network tends to be stable. Under the same SNR, the throughput of the proposed scheme is always much higher than that of the system without IR, which proves the superiority of the proposed scheme.

The change of system throughput with κ is shown in Figure 8. With the increase of κ, the throughput of the SN increases first and then decreases, but the overall change is limited. Under different SNR, the κ value corresponding to

Table 2: SINR of the schemas.

SINR	NIR
$\gamma_{x_1}^{R_1}$	$\rho_T\lvert h_{PR_1}\rvert^2/\left(\kappa\rho_T\lvert h_{SR_1}\rvert^2+1\right)$
$\gamma_{x_2}^{R_1}$	$\kappa\rho_T\lvert h_{SR_1}\rvert^2$
$\gamma_{x_1}^{PU}$	$\psi\rho_{R_1}\lvert h_{R_1P}\rvert^2/\left((1-\psi)\rho_{R_1}\lvert h_{R_1P}\rvert^2+1\right)$
$\gamma_{x_1}^{SU}$	$\psi\rho_{R_1}\lvert h_{R_1S}\rvert^2/\left((1-\psi)\rho_{R_1}\lvert h_{R_1S}\rvert^2+1\right)$
$\gamma_{x_2}^{SU}$	$(1-\psi)\rho_{R_1}\lvert h_{R_1S}\rvert^2$

the optimal throughput is different, but exactly equal to the result of (23). In addition, the larger the SNR, the larger the κ value corresponding to the maximum system throughput. Compared with the network without IR, this scheme can obtain better interrupt performance. Feedback time δ also affects the throughput of the system. As the feedback time becomes longer, the throughput decreases.

Figure 9 shows the variation of the throughput of the SN with power distribution coefficient ψ. In a word, with the increase of ψ and with the same SNR, the throughput of the SN increases first and then decreases. However, the proposed scheme with IR has little change in throughput. The ψ values corresponding to the minimum power outage probability are equal under different SNR (simulation results show that the minimum power outage probability ψ value is 0.3023). This result is consistent with (23). With different SNR, the change of δ has little influence on throughput, indicating that the SNR is the main factor affecting the system throughput compared with δ.

5.3. Optimum Power Allocation. In Figure 10, the Monte Carlo method is used to simulate the optimized power distribution schema and average power distribution schema in this paper. The tradeoff performance of outage probability and throughput of SN is compared. As can be seen from the change in Figure 10, under the same power distribution schema, the tradeoff performance between the outage probability and throughput of the proposed scheme is always better than that of the scheme without IR. In addition, under the same SNR, the outage probability and throughput performance of the optimized scheme are better than that of the average power allocation scheme. When the SNR is greater than 30 dB, the $\mathrm{Thr_{ID}}$/Pout value of the average power distribution scheme tends to be stable, while that of the optimized scheme can always increase with the increase of the SNR.

6. Conclusion

In this article, we propose a CR-NOMA network model based on IR. The expression of outage probability and throughput of the SN is derived. The variation of SNR, power distribution factor κ, and ψ all affect the performance of the SN. To improve the tradeoff performance between the outage probability and throughput of the SN, the values of κ and ψ are optimized. And the simulation results show that the outage performance of the system is indeed improved compared with the average power distribution schema. Furthermore, compared with the network without IR, it is shown that the proposed scheme using IR protocol can improve the reliability of the network. The results of this study indicate that the proposed scheme is a promising approach to improve the performance of SN without affecting the performance of PN.

Appendix

A. Proof of Theorem 1

The expression (10) can be rewritten as (A.1). And then the expression (11) can be rewritten as

$$\begin{aligned}\mathrm{Pout1} &= 1-\Pr\left\{\gamma_{x_1}^{R_1}\geq\gamma_{th}^{x_1},\gamma_{x_2}^{R_1}\geq\gamma_{th}^{x_2}\right\}\\ &= 1-\Pr\left\{\frac{\rho_T\lvert h_{PR_1}\rvert^2}{\kappa\rho_T\lvert h_{SR_1}\rvert^2+1}\geq\gamma_{th}^{x_1},\kappa\rho_T\lvert h_{SR_1}\rvert^2\geq\gamma_{th}^{x_2}\right\}\\ &= 1-\int_{\gamma_{th}^{x_2}/\kappa\rho_T}^{\infty}\left(e^{-\left(x\kappa\rho_T\gamma_{th}^{x_1}+\gamma_{th}^{x_1}\right)/\rho_T\lambda_{PR_1}}\right)\left(\frac{1}{\lambda_{SR_1}}e^{-x/\lambda_{SR_1}}\right)\\ &\quad\cdot dx = 1-\frac{\lambda_{PR_1}}{\lambda_{PR_1}+\kappa\lambda_{SR_1}\gamma_{th}^{x_1}}e^{-\left(\left(\gamma_{th}^{x_1}+\gamma_{th}^{x_1}\gamma_{th}^{x_2}\right)/\rho_T\lambda_{PR_1}\right)-\left(\gamma_{th}^{x_2}/\kappa\rho_T\lambda_{SR_1}\right)},\end{aligned}\tag{A.1}$$

$$\begin{aligned}\mathrm{Pout2\_PU} &= 1-\Pr\left\{\gamma_{x_1}^{\mathrm{PU}}\geq\gamma_{th}^{x_1}\right\}\\ &= 1-\Pr\left\{\frac{\psi\rho_{R_1}\lvert h_{R_1P}\rvert^2}{(1-\psi)\rho_{R_1}\lvert h_{R_1P}\rvert^2+1}\geq\gamma_{th}^{x_1}\right\}\\ &= 1-\Pr\left\{\lvert h_{R_1P}\rvert^2\geq\frac{\gamma_{th}^{x_1}}{\lambda_{R_1P}\psi\left(1+\gamma_{th}^{x_1}\right)\rho_{R_1}-\gamma_{th}^{x_1}\rho_{R_1}\lambda_{R_1P}}\right\}\\ &= 1-e^{-\gamma_{th}^{x_1}/\left(\lambda_{R_1P}\psi\left(1+\gamma_{th}^{x_1}\right)\rho_{R_1}-\gamma_{th}^{x_1}\rho_{R_1}\lambda_{R_1P}\right)}.\end{aligned}\tag{A.2}$$

Note that (A.2) is derived on the condition of $\psi>(\gamma_{th}^{x_1}/(1+\gamma_{th}^{x_1}))$ as the outage probability ranges from 0 to 1. Otherwise, the outage probability is equal to 1. Combining (A.1) and (A.2), the outage probability of the PN can be rewritten as

$$\begin{aligned}&\mathrm{Pout,\ PU} = \mathrm{Pout1}+(1-\mathrm{Pout1})\times\mathrm{Pout2\_PU}\\ &=\begin{cases}1-\dfrac{\lambda_{PR_1}e^{-\left(\left(\gamma_{th}^{x_1}+\gamma_{th}^{x_1}\gamma_{th}^{x_2}\right)/\rho_T\lambda_{PR_1}\right)-\left(\gamma_{th}^{x_2}/\kappa\rho_T\lambda_{SR_1}\right)-\left(\gamma_{th}^{x_1}/\left(\lambda_{R_1P}\psi\left(1+\gamma_{th}^{x_1}\right)\rho_{R_1}-\gamma_{th}^{x_1}\rho_{R_1}\lambda_{R_1P}\right)\right)}}{\lambda_{PR_1}+\kappa\lambda_{SR_1}\gamma_{th}^{x_1}}, & \psi>\dfrac{\gamma_{th}^{x_1}}{1+\gamma_{th}^{x_1}},\\ 1, \quad \text{otherwise.}\end{cases}\end{aligned}\tag{A.3}$$

The proof is completed.

B. Proof of Theorem 2

According to the calculation result of (A.1), the outage probability of R1 can be expressed as

$$Pout1 = 1 - \frac{\lambda_{PR_1}}{\lambda_{PR_1} + \kappa\lambda_{SR_1}\gamma_{th}^{x_1}} e^{-\gamma_{th}^{x_1} + \gamma_{th}^{x_1}\gamma_{th}^{x_2}/\rho_T\lambda_{PR_1} - \gamma_{th}^{x_2}/\kappa\rho_T\lambda_{SR_1}}. \tag{A.4}$$

The expression (13) can be rewritten as

$$\begin{aligned}\text{Pout2\_SU} = 1 &- \Pr\left\{\gamma_{x_1}^{SU} \geq \gamma_{th}^{x_1}, \gamma_{x_2}^{SU} \geq \gamma_{th}^{x_2}\right\} \\ &- \left(\left(1 - \Pr\left\{\gamma_{x_1}^{SU} \geq \gamma_{th}^{x_1}, \gamma_{x_2}^{SU} \geq \gamma_{th}^{x_2}\right\}\right)\right. \\ &\left.\times \Pr\left\{\gamma_{x_2}^{R_2} \geq \gamma_{th}^{x_2}, \gamma_{x_2}^{R_2 \longrightarrow SU} \geq \gamma_{th}^{x_2}\right\}\right).\end{aligned} \tag{A.5}$$

We define $\Pr\{\gamma_{x_1}^{SU} \geq \gamma_{th}^{x_1}, \gamma_{x_2}^{SU} \geq \gamma_{th}^{x_2}\}$ as $H1$ and $\Pr\{\gamma_{x_2}^{R_2} \geq \gamma_{th}^{x_2}, \gamma_{x_2}^{R_2 \longrightarrow SU} \geq \gamma_{th}^{x_2}\}$ as $H2$. Then, the following results can be obtained

$$\begin{aligned}H1 &= \Pr\left\{\frac{\psi\rho_{R_1}|h_{R_1S}|^2}{(1-\psi)\rho_{R_1}|h_{R_1S}|^2 + 1} \geq \gamma_{th}^{x_1}, (1-\psi)\rho_{R_1}|h_{R_1S}|^2 \geq \gamma_{th}^{x_2}\right\} \\ &= \Pr\left\{|h_{R_1S}|^2 \geq \frac{\gamma_{th}^{x_1}}{\psi\rho_{R_1} - \gamma_{th}^{x_1}(1-\psi)\rho_{R_1}}, |h_{R_1S}|^2 \geq \frac{\gamma_{th}^{x_2}}{(1-\psi)\rho_{R_1}}\right\} \\ &= e^{-\theta/\rho_{R_1}\lambda_{R_1S}}, \theta = \max\left(\frac{\gamma_{th}^{x_1}}{\psi - \gamma_{th}^{x_1}(1-\psi)}, \frac{\gamma_{th}^{x_2}}{(1-\psi)}\right),\end{aligned} \tag{A.6}$$

$$\begin{aligned}H2 &= \Pr\left\{\frac{(1-\psi)\rho_{R_1}|h_{R_1R_2}|^2}{\psi\rho_{R_1}|h_{R_1R_2}|^2 + 1} \geq \gamma_{th}^{x_2}, \min\left(\frac{Q_{th}}{|h_{SP}|^2}, \rho_{R_2}\right)|h_{R_2S}|^2 \geq \gamma_{th}^{x_2}\right\} \\ &== e^{-\left(1/\lambda_{R_1R_2}\right)\left(\gamma_{th}^{x_2}/\left((1-\psi)\rho_{R_1} - \gamma_{th}^{x_2}\psi\rho_{R_1}\right)\right)} \\ &\quad\times \int_{\gamma_{th}^{x_2}/\rho_{R2}}^{\infty} \frac{1}{\lambda_{R_2S}} e^{-x/\lambda_{R_2S}} \int_0^{Q_{th}x/\gamma_{th}^{x_2}} \frac{1}{\lambda_{SP}} e^{-y/\lambda_{SP}} dydx \\ &= e^{-\left(1/\lambda_{R_1R_2}\right)\left(\gamma_{th}^{x_2}/\left((1-\psi)\rho_{R_1} - \gamma_{th}^{x_2}\psi\rho_{R_1}\right)\right) - \left(\gamma_{th}^{x_2}/\lambda_{R_2S}\rho_{R_2}\right)} \\ &\quad\cdot \left(1 - \left(\frac{\lambda_{SP}\gamma_{th}^{x_2}}{\lambda_{SP}\gamma_{th}^{x_2} + Q_{th}\lambda_{R_2S}} e^{-Q_{th}\gamma_{th}^{x_2}/\lambda_{SP}\gamma_{th}^{x_2}\rho_{R2}}\right)\right).\end{aligned} \tag{A.7}$$

Note that (A.7) is derived on the condition of $\psi < (1/(1 + \gamma_{th}^{x_2}))$ as the outage probability ranges from 0 to 1. Otherwise, the outage probability is equal to 1. Substitute (A.6) and (A.7) into (A.5), the outage probability of the second phase of the SN is given as

$$\begin{aligned}\text{Pout2\_SU} &= 1 - H1 - (1 - H1) \times H2 \\ &= (1 - H1)(1 - H2) = \left(1 - e^{-\theta/\rho_{R_1}\lambda_{R_1S}}\right) \\ &\quad\times \left(1 - e^{-\left(1/\lambda_{R_1R_2}\right)\left(\gamma_{th}^{x_2}/(1-\psi)\rho_{R_1} - \gamma_{th}^{x_2}\psi\rho_{R_1}\right) - \left(\gamma_{th}^{x_2}/\lambda_{R_2S}\rho_{R_2}\right)}\right. \\ &\quad\left.\times \left(1 - \left(\frac{\lambda_{SP}\gamma_{th}^{x_2}}{\lambda_{SP}\gamma_{th}^{x_2} + Q_{th}\lambda_{R_2S}} e^{-Q_{th}\gamma_{th}^{x_2}/\lambda_{SP}\gamma_{th}^{x_2}\rho_{R_2}}\right)\right)\right).\end{aligned} \tag{A.8}$$

Combining (A.4) and (A.8), the system outage probability of the SN using an IR to assist transmission on the condition of $\psi < (1/(1 + \gamma_{th}^{x_2}))$ can be given as

$$\begin{aligned}\text{Pout\_SU} &= \text{Pout1} + (1 - \text{Pout1}) \times \text{Pout2\_SU} \\ &= 1 - \frac{\lambda_{PR_1}}{\lambda_{PR_1} + \kappa\lambda_{SR_1}\gamma_{th}^{x_1}} e^{-\left(\left(\gamma_{th}^{x_1} + \gamma_{th}^{x_1}\gamma_{th}^{x_2}\right)/\rho_T\lambda_{PR_1}\right) - \left(\gamma_{th}^{x_2}/\kappa\rho_T\lambda_{SR_1}\right)} \\ &\quad + \frac{\lambda_{PR_1}}{\lambda_{PR_1} + \kappa\lambda_{SR_1}\gamma_{th}^{x_1}} e^{-\left(\left(\gamma_{th}^{x_1} + \gamma_{th}^{x_1}\gamma_{th}^{x_2}\right)/\rho_T\lambda_{PR_1}\right) - \left(\gamma_{th}^{x_2}/\kappa\rho_T\lambda_{SR_1}\right)} \\ &\quad\times \left(1 - e^{-\theta/\rho_{R_1}\lambda_{R_1S}}\right) \\ &\quad\times \left(1 - e^{-\left(1/\lambda_{R_1R_2}\right)\left(\gamma_{th}^{x_2}/\left((1-\psi)\rho_{R_1} - \gamma_{th}^{x_2}\psi\rho_{R_1}\right)\right) - \left(\gamma_{th}^{x_2}/\lambda_{R_2S}\rho_{R_2}\right)}\right. \\ &\quad\left.\times \left(1 - \left(\frac{\lambda_{SP}\gamma_{th}^{x_2}}{\lambda_{SP}\gamma_{th}^{x_2} + Q_{th}\lambda_{R_2S}} e^{-Q_{th}\gamma_{th}^{x_2}/\lambda_{SP}\gamma_{th}^{x_2}\rho_{R_2}}\right)\right)\right).\end{aligned} \tag{A.9}$$

After simplification, the outage probability of the SN using an IR is shown as (14).

The proof is completed.

C. Proof of Theorem 4

In the schema without IR, PT and ST send a message to R1, respectively. Then, R1 relays the decoded and reencoded information to PU and SU. For comparison purposes, let NIR represent the scheme without IR. Assume that this scheme has the same channel representation as the scheme mentioned in this article. Based on SIC technique, the SINR of NIR are listed in Table 2.

Similarly, according to the calculation result of (A.1), the outage probability of R1 in the schema without IR is

$$\text{Pout1} = 1 - \frac{\lambda_{PR_1}}{\lambda_{PR_1} + \kappa\lambda_{SR_1}\gamma_{th}^{x_1}} e^{-\left(\left(\left(\gamma_{th}^{x_1} + \gamma_{th}^{x_1}\gamma_{th}^{x_2}\right)/\rho_T\lambda_{PR_1}\right)\right) - \left(\gamma_{th}^{x_2}/\kappa\rho_T\lambda_{SR_1}\right)}. \tag{A.10}$$

Since the presence or absence of an IR does not affect the outage probability of the PN, the outage probability of the second phase of the SN is discussed. Refer to the expressions for $\gamma_{x_1}^{\text{SU}}$ and $\gamma_{x_2}^{\text{SU}}$; the closed-form expression of the SN can be expressed as

$$\begin{aligned}\text{Pout2\_NIR} &= 1 - \Pr\left\{\gamma_{x_1}^{\text{SU}} \geq \gamma_{th}^{x_1}, \gamma_{x_2}^{\text{SU}} \geq \gamma_{th}^{x_2}\right\} \\ &= 1 - \Pr\left\{\frac{\psi\rho_{R_1}|h_{R_1S}|^2}{(1-\psi)\rho_{R_1}|h_{R_1S}|^2 + 1} \geq \gamma_{th}^{x_1}, (1-\psi)\rho_{R_1}|h_{R_1S}|^2 \geq \gamma_{th}^{x_2}\right\} \\ &= 1 - \Pr\left\{|h_{R_1S}|^2 \geq \frac{\gamma_{th}^{x_1}}{\psi\rho_{R_1} - \gamma_{th}^{x_1}(1-\psi)\rho_{R_1}}, |h_{R_1S}|^2 \geq \frac{\gamma_{th}^{x_2}}{(1-\psi)\rho_{R_1}}\right\} \\ &= 1 - e^{-\theta/\rho_{R_1}\lambda_{R_1S}},\end{aligned} \tag{A.11}$$

where $\theta = \max\left(\gamma_{th}^{x_1}/(\psi - \gamma_{th}^{x_1}(1-\psi)), \gamma_{th}^{x_2}/(1-\psi)\right)$.

Combining (A.10) and (A.11), the outage probability of the network without IR can be expressed as (20).

The proof is completed.

D. Proof of Theorem 6

Taking the partial derivative of the objective function in (23) on κ, we have

$$g(\kappa) = \frac{\partial\left(-\left(1/\left(\lambda_{PR_1} + \kappa\lambda_{SR_1}\gamma_{th}^{x_1}\right)\right)e^{-\gamma_{th}^{x_2}/\kappa\rho_T\lambda_{SR_1}}\right)}{\partial\kappa} = \frac{\lambda_{SR_1}\gamma_{th}^{x_1}}{\left(\lambda_{PR_1} + \kappa\lambda_{SR_1}\gamma_{th}^{x_1}\right)^2}e^{-\gamma_{th}^{x_2}/\kappa\rho_T\lambda_{2r}} - \frac{1}{\lambda_{PR_1} + \kappa\lambda_{SR_1}\gamma_{th}^{x_1}} \times \frac{\gamma_{th}^{x_2}}{\kappa^2\rho_T\lambda_{SR_1}}e^{-\gamma_{th}^{x_2}/\kappa\rho_T\lambda_{SR_1}} = \frac{1}{\lambda_{PR_1} + \kappa\lambda_{SR_1}\gamma_{th}^{x_1}}e^{-\gamma_{th}^{x_2}/\kappa\rho_T\lambda_{SR_1}} \times \left(\frac{\lambda_{SR_1}\gamma_{th}^{x_1}}{\lambda_{PR_1} + \kappa\lambda_{SR_1}\gamma_{th}^{x_1}} - \frac{\gamma_{th}^{x_2}}{\kappa^2\rho_T\lambda_{SR_1}}\right). \tag{A.12}$$

Let $g(\kappa) = 0$, we can get

$$\frac{\gamma_{th}^{x_2}}{\kappa^2\rho_T\lambda_{SR_1}} = \frac{\lambda_{SR_1}\gamma_{th}^{x_1}}{\lambda_{PR_1} + \kappa\lambda_{SR_1}\gamma_{th}^{x_1}}. \tag{A.13}$$

Let $A = \gamma_{th}^{x_2}/\rho_T\lambda_{SR_1}$, $B = \lambda_{SR_1}\gamma_{\text{th}}^{x_1}$, (A.13) can be written as

$$\frac{A}{\kappa^2} = \frac{B}{\lambda_{PR_1} + \kappa B}. \tag{A.14}$$

According to the properties of the equation, (A.14) can also be expressed as $B\kappa^2 - A\kappa B - A\lambda_{PR_1} = 0$. Since $\kappa > 0$ and $\Delta = \sqrt{(AB)^2 + 4AB\lambda_{PR_1}} > 0$ are always correct, the objective function gets the minimum value when $\kappa^* = AB + \Delta/2B$ without considering the condition constraint. Constrained by $C1$ and $C2$, we obtain that the range of κ is $(\gamma_{th}^{x_2}/(\rho_T|h_{SR_1}|^2)) \le \kappa \le ((\rho_T|h_{PR_1}|^2 - \gamma_{th}^{x_1})/(\gamma_{th}^{x_1}\rho_T|h_{SR_1}|^2))$. Therefore, the range of κ can be expressed as $\kappa \in [\kappa_{\min}, \kappa_{\max}]$. When $\kappa^* \in [\kappa_{\min}, \kappa_{\max}]$, the solution of the first-phase optimization problem is $\kappa = \kappa^*$. If κ is less than $\kappa_{\min}$, within the value range of κ, the objective function decreases as κ increases. In this case, $\kappa = \kappa_{\min}$. Otherwise, $\kappa = \kappa_{\max}$.

The proof is completed.

E. Proof of Theorem 7

According to (18), the monotonicity of the SN throughput depends on two parts, Pout_SU and $1/e^{-\theta/\rho_{R_1}\lambda_{R_1S}}$. Throughput is negatively correlated with the value of Pout_SU and positively correlated with the value of $1/e^{-\theta/\rho_{R_1}\lambda_{R_1S}}$.

For $1/e^{-\theta/\rho_{R_1}\lambda_{R_1S}}$, as mentioned in (A.11), $\theta = \max(\gamma_{th}^{x_1}/(\psi - \gamma_{th}^{x_1}(1-\psi)), \gamma_{th}^{x_2}/(1-\psi))$; thus, θ can be expressed as

$$\theta = \begin{cases} \dfrac{\gamma_{th}^{x_1}}{\psi - \gamma_{th}^{x_1}(1-\psi)}, & \psi < \dfrac{\gamma_{th}^{x_1} + \gamma_{th}^{x_1}\gamma_{th}^{x_2}}{\gamma_{th}^{x_2} + \gamma_{th}^{x_1}\gamma_{th}^{x_2} + \gamma_{th}^{x_1}}, \\ \dfrac{\gamma_{th}^{x_2}}{(1-\psi)}, & \psi \ge \dfrac{\gamma_{th}^{x_1} + \gamma_{th}^{x_1}\gamma_{th}^{x_2}}{\gamma_{th}^{x_2} + \gamma_{th}^{x_1}\gamma_{th}^{x_2} + \gamma_{th}^{x_1}}. \end{cases} \tag{A.15}$$

When $\psi \ge ((\gamma_{th}^{x_1} + \gamma_{th}^{x_1}\gamma_{th}^{x_2})/(\gamma_{th}^{x_2} + \gamma_{th}^{x_1}\gamma_{th}^{x_2} + \gamma_{th}^{x_1}))$, θ decreases monotonically while when $\psi < \gamma_{th}^{x_1} + \gamma_{th}^{x_1}\gamma_{th}^{x_2}/\gamma_{th}^{x_2} + \gamma_{th}^{x_1}\gamma_{th}^{x_2} + \gamma_{th}^{x_1}$, it is increasing. And so is $1/e^{-\theta/\rho_{R_1}\lambda_{R_1S}}$.

Set $K1 = 1 - ((\lambda_{SP}\gamma_{th}^{x_2}/(\lambda_{SP}\gamma_{th}^{x_2} + Q_{th}\lambda_{R_2S}))e^{-Q_{th}\gamma_{th}^{x_2}/\lambda_{SP}\gamma_{th}^{x_2}\rho_{R_2}})$. For Pout_SU, after removing the effect of constant terms, the increase or decrease in Pout_SU can be expressed as the increase or decrease in f, where f stands for $(1 - e^{-\theta/\rho_{R_1}\lambda_{R_1S}}) \times (1 - K1 \times e^{-(1/\lambda_{R_1R_2})(\gamma_{th}^{x_2}/((1-\psi)\rho_{R_1} - \gamma_{th}^{x_2}\psi\rho_{R_1}))})$. When the power distribution factor satisfies $\psi \ge ((\gamma_{th}^{x_1} + \gamma_{th}^{x_1}\gamma_{th}^{x_2})/(\gamma_{th}^{x_2} + \gamma_{th}^{x_1}\gamma_{th}^{x_2} + \gamma_{th}^{x_1}))$, f is the product of two increasing functions, $(\partial f/\partial\psi) > 0$. Therefore, f increases monotonically in the domain. Similarly, when $\psi < ((\gamma_{th}^{x_1} + \gamma_{th}^{x_1}\gamma_{th}^{x_2})/(\gamma_{th}^{x_2} + \gamma_{th}^{x_1}\gamma_{th}^{x_2} + \gamma_{th}^{x_1}))$, it can be proved numerically $(\partial f/\partial\psi) < 0$. Therefore, f decreases monotonically. As a consequence, the minimum value is obtained when $\psi = (\gamma_{th}^{x_1} + \gamma_{th}^{x_1}\gamma_{th}^{x_2})/(\gamma_{th}^{x_2} + \gamma_{th}^{x_1}\gamma_{th}^{x_2} + \gamma_{th}^{x_1})$.

Therefore, the throughput of the SN increases when $\psi < ((\gamma_{th}^{x_1} + \gamma_{th}^{x_1}\gamma_{th}^{x_2})/(\gamma_{th}^{x_2} + \gamma_{th}^{x_1}\gamma_{th}^{x_2} + \gamma_{th}^{x_1}))$, while it decreases when $\psi \ge ((\gamma_{th}^{x_1} + \gamma_{th}^{x_1}\gamma_{th}^{x_2})/(\gamma_{th}^{x_2} + \gamma_{th}^{x_1}\gamma_{th}^{x_2} + \gamma_{th}^{x_1}))$. Similarly, Pout_SU and 1/Pout_SU are negatively correlated. In other words, Thr_{ID} and 1/Pout are equally distributed.

The proof is completed.

F. Proof of Theorem 8

According to $C1$ in (24), the feasible range of ψ is derived by

$$\psi \ge \underbrace{\frac{\gamma_{th}^{x_1}}{\rho_{R_1}|h_{R_1P}|^2 + \gamma_{th}^{x_1}\rho_{R_1}|h_{R_1P}|^2}}_{\chi} + \frac{\gamma_{th}^{x_1}}{1 + \gamma_{th}^{x_1}} > \frac{\gamma_{th}^{x_1}}{1 + \gamma_{th}^{x_1}}. \tag{A.16}$$

Taking $C2$ in (24) into consideration, it should be noted that the solution $\psi \in [\psi_{\min}, \psi_{\max}] = [\chi, 1/(1 + \gamma_{th}^{x_2})]$ is feasible if and only if $\chi < (1/(1 + \gamma_{th}^{x_2}))$. Otherwise, $\psi = \varnothing$. In this case, the value of the power distribution factor ψ is χ to ensure the normal communication of the PN.

When $\chi < (1/(1 + \gamma_{th}^{x_2}))$, to determine whether $(\gamma_{th}^{x_1} + \gamma_{th}^{x_1}\gamma_{th}^{x_2})/(\gamma_{th}^{x_2} + \gamma_{th}^{x_1}\gamma_{th}^{x_2} + \gamma_{th}^{x_1})$ is in the range of ψ, we do the following subtraction:

$$\frac{\gamma_{th}^{x_1} + \gamma_{th}^{x_1}\gamma_{th}^{x_2}}{\gamma_{th}^{x_2} + \gamma_{th}^{x_1}\gamma_{th}^{x_2} + \gamma_{th}^{x_1}} - \frac{\gamma_{th}^{x_1}}{1 + \gamma_{th}^{x_1}} = \frac{\left(\gamma_{th}^{x_1} + \gamma_{th}^{x_1}\gamma_{th}^{x_2}\right)\left(1 + \gamma_{th}^{x_1}\right) - \gamma_{th}^{x_1}\left(\gamma_{th}^{x_1} + \gamma_{th}^{x_2} + \gamma_{th}^{x_1}\gamma_{\text{th}}^{x_2}\right)}{\left(\gamma_{th}^{x_1} + \gamma_{th}^{x_2} + \gamma_{th}^{x_1}\gamma_{th}^{x_2}\right)\left(1 + \gamma_{th}^{x_1}\right)} > 0, \tag{A.17}$$

$$\frac{\gamma_{th}^{x_1}+\gamma_{th}^{x_1}\gamma_{th}^{x_2}}{\gamma_{th}^{x_2}+\gamma_{th}^{x_1}\gamma_{th}^{x_2}+\gamma_{th}^{x_1}}-\frac{1}{1+\gamma_{th}^{x_2}} = \frac{\left(\gamma_{th}^{x_1}+\gamma_{th}^{x_1}\gamma_{th}^{x_2}\right)\left(1+\gamma_{th}^{x_2}\right)-\left(\gamma_{th}^{x_1}+\gamma_{th}^{x_2}+\gamma_{th}^{x_1}\gamma_{th}^{x_2}\right)}{\left(\gamma_{th}^{x_1}+\gamma_{th}^{x_2}+\gamma_{th}^{x_1}\gamma_{th}^{x_2}\right)\left(1+\gamma_{th}^{x_2}\right)}. \tag{A.18}$$

It can be obtained from (A.17) that $((\gamma_{th}^{x_1}+\gamma_{th}^{x_1}\gamma_{th}^{x_2})/(\gamma_{th}^{x_2}+\gamma_{th}^{x_1}\gamma_{th}^{x_2}+\gamma_{th}^{x_1}))>(\gamma_{th}^{x_1}/(1+\gamma_{th}^{x_1}))$. In addition, when $\gamma_{th}^{x_1}\le(1/(1+\gamma_{th}^{x_1}))$, (A.18) is negative. In this case, if $\gamma_{th}^{x_1}<(\chi\gamma_{th}^{x_2}/((1-\chi)(1+\gamma_{th}^{x_2})))$, $((\gamma_{th}^{x_1}+\gamma_{th}^{x_1}\gamma_{th}^{x_2})/(\gamma_{th}^{x_2}+\gamma_{th}^{x_1}\gamma_{th}^{x_2}+\gamma_{th}^{x_1}))\in[\psi_{\min},\psi_{\max}]$. Therefore, if and only if $\chi<(1/(1+\gamma_{th}^{x_2}))$, the optimized power distribution factor can be expressed as

$$\psi^*=\begin{cases}\chi, & \gamma_{th}^{x_1}<\dfrac{\chi\gamma_{th}^{x_2}}{(1-\chi)\left(1+\gamma_{th}^{x_2}\right)},\\ \dfrac{\gamma_{th}^{x_1}+\gamma_{th}^{x_1}\gamma_{th}^{x_2}}{\gamma_{th}^{x_2}+\gamma_{th}^{x_1}\gamma_{th}^{x_2}+\gamma_{th}^{x_1}}, & \dfrac{\chi\gamma_{th}^{x_2}}{(1-\chi)\left(1+\gamma_{th}^{x_2}\right)}<\gamma_{th}^{x_1}\le\dfrac{1}{1+\gamma_{th}^{x_2}},\\ \dfrac{1}{1+\gamma_{th}^{x_2}}, & \gamma_{th}^{x_1}>\dfrac{1}{1+\gamma_{th}^{x_2}}.\end{cases} \tag{A.19}$$

Data Availability

No data were used to support this study.

Conflicts of Interest

There are no conflicts of interest regarding the publication of this article.

Acknowledgments

This work was supported by the Natural Science Foundation of Shandong Province, under Grant ZR2018MF002, and in part by the National Natural Science Foundation of China, under Grant 61902205.

References

[1] J. Zhao, Z. Dong, H. Qu, and L. Lu, "Allocation algorithm for maximizing spectrum resource utilization on D2D communication in Internet of Vehicles," *Application Research of Computers*, vol. 38, no. 7, pp. 2144–2148, 2021.

[2] J. Navarro-Ortiz, P. Romero-Diaz, S. Sendra, P. Ameigeiras, J. J. Ramos-Munoz, and J. M. Lopez-Soler, "A survey on 5G usage scenarios and traffic models," *IEEE Communication Surveys and Tutorials*, vol. 22, no. 2, pp. 905–929, 2020.

[3] M. Agiwal, H. Kwon, S. Park, and H. Jin, "A survey on 4G-5G dual connectivity: road to 5G implementation," *IEEE Access*, vol. 9, pp. 16193–16210, 2021.

[4] A. Yadav, C. Quan, P. K. Varshney, and H. V. Poor, "On performance comparison of multi-antenna HD-NOMA, SCMA, and PD-NOMA schemes," *IEEE Wireless Communications Letters*, vol. 10, no. 4, pp. 715–719, 2021.

[5] J. Zeng, T. Lv, R. P. Liu et al., "Investigation on evolving single-carrier NOMA into multi-carrier NOMA in 5G," *IEEE Access*, vol. 6, pp. 48268–48288, 2018.

[6] S. M. R. Islam, N. Avazov, O. A. Dobre, and K. S. Kwak, "Power-domain non-orthogonal multiple access (NOMA) in 5G systems: potentials and challenges," *IEEE Communication Surveys and Tutorials*, vol. 19, no. 2, pp. 721–742, 2017.

[7] X. Li, J. Li, Y. Liu, Z. Ding, and A. Nallanathan, "Residual transceiver hardware impairments on cooperative NOMA networks," *IEEE Transactions on Wireless Communications*, vol. 19, no. 1, pp. 680–695, 2020.

[8] H. Liu, G. Li, X. Li, Y. Liu, G. Huang, and Z. Ding, "Effective capacity analysis of STAR-RIS assisted NOMA networks," *IEEE Wireless Communications Letters*, vol. 11, no. 9, pp. 1930–1934, 2022.

[9] Y. Zhang, Y. Zhang, X. Zhao et al., "Power allocation algorithms for stable successive interference cancellation in millimeter wave NOMA systems," *IEEE Transactions on Vehicular Technology*, vol. 70, no. 6, pp. 5833–5847, 2021.

[10] S. Pazhayakandathil, D. Sukumaran, and H. Abdul, "A Novel Low Complexity Power Allocation Algorithm for Downlink NOMA Networks," *2018 IEEE Recent Advances in Intelligent Computational Systems (RAICS)*, pp. 36–40, 2018.

[11] M. Karimi, S. M. S. Sadough, and M. Torabi, "Improved joint spectrum sensing and power allocation for cognitive radio networks using probabilistic spectrum access," *IEEE Systems Journal*, vol. 13, no. 4, pp. 3716–3723, 2019.

[12] K. K. Singh, P. Yadav, A. Singh, G. Dhiman, and K. Cengiz, "Cooperative spectrum sensing optimization for cognitive radio in 6 G networks," *Computers and Electrical Engineering*, vol. 95, no. 5, article 107378, 2021.

[13] D. -T. Do, M. -S. V. Nguyen, F. Jameel, R. Jäntti, and I. S. Ansari, "Performance evaluation of relay-aided CR-NOMA for beyond 5G communications," *IEEE Access*, vol. 8, pp. 134838–134855, 2020.

[14] S. Arzykulov, A. Celik, G. Nauryzbayev, and A. M. Eltawil, "UAV-assisted cooperative & cognitive NOMA: deployment, clustering, and resource allocation," *IEEE Transactions on Cognitive Communications and Networking*, vol. 8, no. 1, pp. 263–281, 2022.

[15] D. -T. Do, T. Anh Le, T. N. Nguyen, X. Li, and K. M. Rabie, "Joint impacts of imperfect CSI and imperfect SIC in cognitive radio-assisted NOMA-V2X communications," *Access*, vol. 8, pp. 128629–128645, 2020.

[16] S. Arzykulov, G. Nauryzbayev, A. Celik, and A. M. Eltawil, "Hardware and interference limited cooperative CR-NOMA networks under imperfect SIC and CSI," *IEEE Open Journal of the Communications Society*, vol. 2, pp. 1473–1485, 2021.

[17] A. -T. Le and D. -T. Do, "CR-NOMA networks over Nakagami- Fading: CSI imperfection perspective," *Wireless Communications and Mobile Computing*, vol. 2021, Article ID 9915974, 10 pages, 2021.

[18] C. E. Garcia, M. R. Camana, and I. Koo, "Secrecy energy efficiency maximization in an underlying cognitive radio-NOMA system with a cooperative relay and an energy-harvesting user," *Applied Sciences*, vol. 10, no. 10, p. 3630, 2020.

[19] G. Singh and P. Thakur, "Performance analysis of MIMO-based CR–NOMA communication systems," *IET Communications*, vol. 14, no. 16, pp. 2677–2686, 2020.

[20] P. M. Nam, T. T. Duy, P. V. Ca, P. N. Son, and N. H. An, "Outage performance of power beacon-aided multi-hop cooperative cognitive radio protocol under constraint of interference and hardware noises," *Electronics*, vol. 9, no. 6, p. 1054, 2020.

[21] M. F. Kader, M. B. Shahab, and S. Y. Shin, "Exploiting non-orthogonal multiple access in cooperative relay sharing," *IEEE Communications Letters*, vol. 21, no. 5, pp. 1159–1162, 2017.

[22] M. F. Kader, S. Y. Shin, and V. C. M. Leung, "Full-duplex non-orthogonal multiple access in cooperative relay sharing for 5G systems," *IEEE Transactions on Vehicular Technology*, vol. 67, no. 7, pp. 5831–5840, 2018.

[23] Z. Liu, Z. Li, Y. Cheng, X. Huang, and Q. Chen, "A full-duplex relay selection strategy based on potential game in cognitive cooperative networks," *Concurrency and Computation Practice and Experience*, vol. 31, no. 9, article e4635, 2019.

[24] G. Li, D. Mishra, and H. Jiang, "Cooperative NOMA with incremental relaying: performance analysis and optimization," *IEEE Transactions on Vehicular Technology*, vol. 67, no. 11, pp. 11291–11295, 2018.

[25] K. Reshma and A. V. Babu, "Throughput analysis of energy harvesting enabled incremental relaying NOMA system," *IEEE Communications Letters*, vol. 24, no. 7, pp. 1419–1423, 2020.

[26] A. K. Shukla, V. Singh, P. K. Upadhyay, A. Kumar, and J. M. Moualeu, "Performance analysis of energy harvesting-assisted overlay cognitive NOMA systems with incremental relaying," *IEEE Open Journal of the Communications Society*, vol. 2, pp. 1558–1576, 2021.

[27] L. T. Tu, P. L. Tung, T. Van Chien, T. T. Duy, and N. T. Hoa, "Performance evaluation of incremental relaying in underlay cognitive radio networks with imperfect CSI," in *2020 IEEE Eighth International Conference on Communications and Electronics (ICCE)*, pp. 472–477, Phu Quoc Island, Vietnam, 2021.

[28] Z. Wang and Q. Zhu, "Energy efficiency optimization algorithm of CR-NOMA system based on SWIPT," *Mathematical Problems in Engineering*, vol. 2020, Article ID 6207989, 13 pages, 2020.

[29] Y. J. Zhu, Y. Li, Z. J. Tian, and J. Y. Chen, "Performance of improved decode-and-forward cooperation in low SNR," *Journal on Communications*, vol. 31, no. 2, pp. 81–85, 2010.